Published in final edited form as:
Biomaterials. 2014 August ; 35(25): 6787–6796. doi:10.1016/j.biomaterials.2014.04.083.

Combined use of chondroitinase-ABC, TGF-β1 and collagen crosslinking agent lysyl oxidase to engineer functional neotissues for fibrocartilage repair

Eleftherios A. Makris[1,2,*], **Regina F. MacBarb**[1,*], **Nikolaos K. Paschos**[1], **Jerry C. Hu**[1], and **Kyriacos A. Athanasiou**[1,3]

[1]Department of Biomedical Engineering, University of California Davis, One Shields Avenue, Davis, CA, United States, 95616

[2]Department of Orthopaedic Surgery and Musculoskeletal Trauma, University of Thessaly, Larisa, Greece, 41110

[3]Department of Orthopaedic Surgery, University of California, Davis, Sacramento, CA, United States, 95616

Abstract

Patients suffering from damaged or diseased fibrocartilages currently have no effective long-term treatment options. Despite their potential, engineered tissues suffer from inferior biomechanical integrity and an inability to integrate *in vivo*. The present study identifies a treatment regimen (including the biophysical agent chondroitinase-ABC, the biochemical agent TGF-β1, and the collagen crosslinking agent lysyl oxidase) to prime highly cellularized, scaffold-free neofibrocartilage implants, effecting continued improvement *in vivo*. We show these agents drive *in vitro* neofibrocartilage matrix maturation toward synergistically enhanced Young's modulus and ultimate tensile strength values, which were increased 245% and 186%, respectively, over controls. Furthermore, an *in vitro* fibrocartilage defect model found this treatment regimen to significantly increase the integration tensile properties between treated neofibrocartilage and native tissue. Through translating this technology to an *in vivo* fibrocartilage defect model, our results indicate, for the first time, that a pre-treatment can prime neofibrocartilage for significantly enhanced integration potential *in vivo*, with interfacial tensile stiffness and strength increasing by 730% and 745%, respectively, compared to integration values achieved *in vitro*. Our results suggest that specifically targeting collagen assembly and organization is a powerful means to augment overall neotissue mechanics and integration potential toward improved clinical feasibility.

[*]**Correspondence and reprint requests should be addressed to:** K.A. Athanasiou, Tel.: (530) 754-6645β Fax: (530) 754-5739β athanasiou@ucdavis.edu Department of Biomedical Engineering, University of California Davis, One Shields Ave, Davis, CA 95616.
[*]Indicates co-first authors

Keywords

Fibrocartilage; tissue engineering; integration; collagen crosslinking; lysyl oxidase

1. Introduction

Collagen-rich musculoskeletal soft tissues, such as the knee menisci, intervertebral discs, temporomandibular joint (TMJ) discs, tendons, and ligaments, lack an intrinsic ability to self-repair following disease- or injury-induced degradation. As such, different fibrocartilage repair techniques have been developed, which typically utilize either autograft or allograft tissue, or scaffold-based replacements. However, such approaches are hindered by implant inability to successfully integrate with host tissue [1, 2]. Proper integration is critical to graft success, as it ensures that the implant remains stabilized and is, therefore, able to competently function *in vivo* [3, 4]. With the insufficiency of current grafts, tissue engineering of neofibrocartilage implants that mimic the complex structures of native tissues holds great potential as a long-term clinical solution for acute fibrocartilage injuries and chronic degenerative pathologies [5]. Toward engineering such implants, it is imperative that they are able to withstand the high mechanical loads of joints and, perhaps even more importantly, are strategically engineered to promote integration with the host tissue upon implantation. Without these critical features, they, like current grafts, may likely fail. Thus, it is critical that treatment modalities are developed that specifically target 1) the maturation and extracellular matrix (ECM) organization, and 2) the integration potential of engineered fibrocartilage implants.

The four most common factors that may either directly or indirectly impede proper fibrocartilage integration are: 1) the avascularity of the host tissue [6], 2) cell death at the periphery of the defect [7], 3) hindrance of cellular migration due to a dense collagen matrix at the wound edge [8], and 4) the lack of stabilizing collagen crosslinks at the native-to-implant interface [9]. Together, these factors result in a metabolically inactive wound edge that limits both matrix synthesis and crosslink formation, hindering integration with any type of implant [10]. Various methods have been developed in an attempt to overcome the yet unresolved hurdle of integration. For instance, biological tissue adhesives have been used at the integration interface [11, 12] as well as enzymatic degradation to temporarily reduce the amount of negatively charged proteoglycans at surfaces of the graft and host tissues [13, 14]. While such methods have had a beneficial effect toward encouraging integration, a stable, biomechanically robust integration interface, able to withstand the complex distribution of forces experienced by fibrocartilaginous tissues, has yet to be achieved.

A self-assembling process has been developed to generate highly cellularized and metabolically active neotissues [15], which may aid in integration upon implantation. Specifically, seeding high-density co-cultures of meniscus cells (MC) and articular chondrocytes (AC) into non-adherent agarose wells promotes the development of neofibrocartilage in a manner akin to native morphogenesis [16, 17]. Past work has identified several exogenous factors to enhance the overall functional properties of self-assembled neotissue, including the bioactive agent transforming growth factor-β1 (TGF-β1)

and the biophysical agent chondroitinase-ABC (C-ABC) [18, 19]. While combined use of these factors has been found to enhance neotissue functional properties through increased collagen content, density, and fibril diameter [20, 21], their tensile properties remain inferior to those of native tissue. Thus, efforts to further promote *in vitro* tissue maturation in addition to enhancing integration potential are necessary to generate mechanically robust neofibrocartilage implants able to withstand the high *in vivo* loads of joints.

Promoting collagen crosslinking in neofibrocartilages may provide a viable solution toward furthering *in vitro* maturation as well as facilitating *in vivo* integration with the host tissue. Natively, lysine-derived, covalent pyridinoline (PYR) crosslinks have been shown to be instrumental to development of a mechanically robust collagen matrix [22]. Such crosslinks are formed via the enzyme lysyl oxidase (LOX), which turns amino acid precursors (lysine and hydroxylysine) into mature PYR crosslinks over time [23, 24]. Capitalizing on the potential of promoting the formation of PYR crosslinks, this study employed a combination of stimuli consisting of exogenous LOX, C-ABC, and TGF-β1 to enhance the tensile properties of self-assembled neofibrocartilage implants as well as effect and stabilize their integration with native tissue. This study was conducted in three phases: The objective of Phase 1 was to promote *in vitro* maturation of engineered fibrocartilage. Phase 2 sought to foster the integration between native and self-assembled fibrocartilages *in vitro*. Finally, Phase 3 investigated the potential of a LOX+C-ABC+TGF-β1 pre-treatment to prime neofibrocartilage for enhanced integration *in vivo.* Overall, it was hypothesized that through collagen enhancement and PYR crosslink formation, combined treatment of LOX+C-ABC +TGF-β1 would 1) induce time-dependent maturation and enhance the tensile properties of the neofibrocartilage constructs, 2) promote *in vitro* integration between engineered and native fibrocartilages, and 3) carry over an effect into the *in vivo* environment to further promote such integration.

2. Materials and Methods

2.1. Neofibrocartilage culture & integration

Juvenile bovine AC and MC were isolated and self-assembled at a 50:50 ratio [20]. For Phase 1, constructs were grown and analyzed at t = 6 and 12 wk. For Phases 2 and 3, integration was investigated by press-fitting 3 mm diameter punches of 6-wk-old neofibrocartilage into donut-shaped, 6 mm outer × 3 mm inner diameter native fibrocartilage explants (porcine-derived mandibular disc fibrocartilage), which were cultured for an additional 6 wk either *in vitro* or *in vivo* (Fig. 3). Native-to-native assemblies were likewise created for Phase 2. For both the *in vitro* and *in vivo* integration phases, the integration interface was analyzed at t = 12 wk. To ensure the constructs remained in place, 1 μl of biodegradable cyanoacrylate was applied to the interface at one specific location of both engineered-to-native and native-to-native assemblies, penetrating ~ 2.5% of the thickness of the tissue. Although histology verified the glue to fully degrade prior to testing, all analysis was conducted opposite where the cyanoacrylate glue was administered to ensure any enhancements observed in integration were not related to the affects of the tissue glue.

2.2. Treatments

This study employed a combination of treatments, including LOX, C-ABC, and TGF-β1. For Phase 1, a two-factor, full factorial study design was employed, which included a treatment factor (control, LOX, -β1, and LOX+C-ABC+TGF-β1) and a culture duration factor (t = 6 or 12 wk). LOX was applied continuously at 0.15 ng/ml from t = 7 – 21 d [25], C-ABC was applied at 2 U/ml for 4 hrs at t = 7 d and t = 21 d [20], while TGF-β1 was applied at 10 ng/ml for the entire culture duration [18]. The second phase of this study sought to promote integration between native and engineered fibrocartilages via an *in vitro* model of integration. The same four treatments were used in Phase 2; the only difference being that LOX was applied 2×, from t = 7 – 21 d and again from t = 35 – 49 d (Fig. 3B), prior to engineered-to-native assembly formation. Native-to-native assemblies in Phase 2 were treated with LOX from for 1 wk following assembly formation. The objectives of Phase 3 were 1) to investigate whether subcutaneous implantation of engineered-to-native assemblies into the backs of nude mice would help to further fortify the integration interface area, and 2) if this fortification could be enhanced via use of the LOX+C-ABC+TGF-β1 pre-treatment established in Phase 2. In Phase 3, the three treatment levels were: control, 1× LOX (from t = 7 – 21 d) +C-ABC+TGF-β1, and 2× LOX (from t = 7 – 21 d and t = 35 – 42 d) +C-ABC+TGF -β1. All treatments in Phase 3 were administered to neofibrocartilage during the first 6 wks of culture, prior to formation of the engineered-to-native assemblies (at t = 42 d) and subcutaneous implantation (at t = 43 d) (Fig. 3B).

2.3. Histology

Segments of constructs from Phase 1, as well as of the integration interface from assemblies of Phases 2 and 3, were cyroembedded and sectioned at 14 μm. Following formalin fixation, slides were stained with either Picrosirius Red for total collagen or Safranin-O/Fast Green for GAG [20].

2.4. Biochemistry & HPLC

Construct segments were weighed before and after lyophilization, and then digested in papain [19]. Total collagen content was measured via a chloramine-T hydroxyproline assay using a SIRCOL standard (Accurate Chemical and Scientific Corp., Westbury, NY). GAG content was measured using a dimethylmethylene blue dye-binding assay kit (Biocolor, Newtownabbey, Northern Ireland). Pyridinoline (PYR) collagen crosslink content was analyzed via HPLC using PYR standards (Quidel, San Diego, CA) [26].

2.5. Mechanical testing

An Instron uniaxial testing machine (Model 5565, Canton, MA) was used to measure unconfined, stress-relaxation data of the neotissue from Phase 1, which were fit to a Kelvin solid model to obtain the neotissue's viscoelastic properties at both t = 6 and 12 wk. Specifically, both E_r and the E_i were calculated, as previously described [20]. For tensile testing, dog-bone-shaped samples from Phase 1, and 1 mm wide strips containing the integration interfaces from Phases 2 and 3, were cut, glued to a paper frame at either extremity, and loaded into the grips of a uniaxial testing machine (Test Resources,

Shakopee, MN). A pull-to-failure test was then conducted, from which the E_Y and UTS were obtained [20].

2.6. SEM

Following ethanol dehydration, Phase 1 neotissue samples were critically point dried and gold sputter coated. A Philips XL30 TMP SEM was used to image three separate locations on each sample. ImageJ was used to quantify the collagen fibril density and diameter of each image [27].

2.7. *In vivo* implantation

Nine male athymic mice, 6–8 weeks in age, were obtained in accordance with the Animal Use and Care Administrative Advisory Committee, University of California, Davis. Mice were anesthetized under general anesthesia, after which a 3 mm incision was made, and two subcutaneous pouches were created on either side of the incision, one on each side of the thorax. Each pouch received one engineered-to-native assembly, such that no mouse received two assemblies from the same treatment group (control, 1× LOX+C-ABC+TGF-β1, or 2× LOX+C-ABC+TGF-β1). The incision was then closed using staples; 6 wk post-surgery, the mice were humanely sacrificed, and the tissue harvested and analyzed.

2.8. Statistics

For Phase 1, a one-way ANOVA (n = 6 per group) was used to test the hypothesis that a LOX+C-ABC+TGF-β1 treatment regimen would enhance the *in vitro* maturation and tensile properties of the neofibrocartilage. Separately, to test the hypothesis that treatments and culture durations were both significant factors in promoting neotissue enhancement, a two-way ANOVA (n = 6 per group) was also used to analyze the data from Phase 1. Data that had a positive interaction on an additive scale and resulted in a combined group that was greater than the addition of the two singular treatments were determined to be synergistic. For Phases 2 and 3, one-way ANOVAs (n = 6 per group) were used to determine the effect of the treatment regimen on enhancing the tensile properties of the integration interface. Upon finding significance ($p < 0.05$), a Tukey's HSD *post hoc* test was applied for all Phases. To compare between Phase 2 and Phase 3 results, two-way ANOVA and Student's *t*-test analyses were used. Data from all phases are represented as mean ± standard deviation.

3. Results

3.1. Phase 1: *In vitro* maturation of engineered fibrocartilage

At both t = 6 and 12 wk, self-assembled neofibrocartilage constructs were analyzed biochemically, biomechanically, and via scanning electron microscopy (SEM). All constructs presented with flat, uniform morphology at both t = 6 and 12 wk (Fig. 1A–B), with TGF-β1 and LOX+C-ABC+TGF-β1 constructs having significantly decreased wet weights, and diameters compared to controls at each respective time point (Table 1). Histologically, collagen staining was more dense and uniform in TGF-β1 and LOX+C-ABC +TGF-β1 groups, while glycosaminoglycan (GAG) staining was denser in control and LOX groups at t = 6 wk. Similar results were observed histologically at t = 12 wk; however, GAG staining appeared to increase in both control and LOX groups at this time (Fig. 1A–B).

Biochemical analysis found significantly greater collagen per wet weight (Col/WW) in TGF-β1- and LOX+C-ABC+TGF-β1-treated constructs at both t = 6 and 12 wk compared to LOX and control constructs. Specifically, at t = 6 wk, the LOX+C-ABC+TGF-β1 group exhibited a 180% increase in Col/WW over controls, and at t = 12 wk, a 228% increase over controls was observed in this group (Fig. 2A). In terms of collagen crosslinks, PYR per wet weight (PYR/WW) was found to be significantly greater in both LOX and LOX+C-ABC +TGF-β1 treated constructs at t = 6 wk, with values 1.9- and 2.7-fold those of respective 6 wk controls. By t = 12 wk, the LOX+C-ABC+TGF-β1-treated constructs exhibited significantly greater PYR/WW over all other groups, with a value 3.8-fold those of 12 wk controls (Fig. 2B). GAG per wet weight (GAG/WW), on the other hand, was found to be significantly greater in control and LOX groups compared to TGF-β1 and LOX+C-ABC +TGF-β1 groups at both the 6 and 12 wk time points (Table 1).

Uniaxial tensile testing at t = 6 wk found the LOX+C-ABC+TGF-β1 treatment to synergistically increase both the Young's modulus (E_Y) and ultimate tensile strength (UTS) 202% and 121%, respectively, over 6 wk controls (Fig. 2C–D). These synergistic enhancements were also observed in t = 12 wk constructs, finding the LOX+C-ABC+TGF-β1-treated neofibrocartilage to have E_Y and UTS values 245% and 186%, respectively, over 12 wk controls. Results further found the 12 wk time point to be a significant factor toward enhancing neotissue tensile properties. Stress-relaxation unconfined compressive testing found both the relaxation modulus (E_r) and instantaneous modulus (E_i) to be significantly greater in LOX constructs compared to all other groups at t = 6 wk (Table 1). By t = 12 wk, both control and LOX groups presented with greater E_r and E_i values compared to TGF-β1 and LOX+C-ABC+TGF-β1 constructs.

Neofibrocartilage constructs were imaged via SEM to investigate the effects of the two factors on *in vitro* matrix development and organization (Fig. 1A–B). Results found 6 wk constructs treated with LOX+C-ABC+TGF-β1 to have a denser collagen matrix displaying bundling of fibrils into fibers compared to control constructs, which appeared less dense and with no sign of bundling. By t = 12 wk, while the control matrix remained relatively unaltered, the bundling of fibrils into densely packed and organized fibers was even more evident in LOX+C-ABC+TGF-β1-treated constructs. Quantitative analysis of the SEM images at both 6 and 12 wk found TGF-β1 and LOX+C-ABC+TGF-β1 constructs to have significantly enhanced collagen fibril densities over controls. The LOX+C-ABC+TGF-β1 treatment was further found to significantly increase the collagen fibril diameter by 92% over controls at the 6 wk time point; by the 12 wk time point, these increases were found to be synergistic, with values increased by 104% over 12 wk controls (Fig. 1C–D). Further, the 12 wk time point was again found to be a significant factor toward promoting maturation of the neofibrocartilage matrix in terms of significantly increasing both the fibril density and diameter.

3.2. Phase 2: *In vitro* integration of native and engineered fibrocartilage

Following 6 wk of *in vitro* integration, the integration interface of engineered-to-native and native-to-native assemblies was analyzed histologically and biomechanically. Histological evaluation of the integration interface found both LOX and LOX+C-ABC+TGF-β1

treatments to promote fusion of the interface in engineered-to-native assemblies; control and TGF-β1-treated assemblies, however, showed little to no integration (Fig. 4A). This was also shown biomechanically: both LOX and LOX+C-ABC+TGF-β1 treatments significantly enhanced the integration interface tensile stiffness and strength in engineered-to-native assemblies over controls or C-ABC+TGF-β1-treated constructs (Fig. 4B,C). Specifically, the E_Y and UTS of the integration interface in LOX-treated assemblies were 2.2- and 2.4-fold those of controls, respectively. Similarly, LOX+C-ABC+TGF-β1-treated assemblies presented with integration interface E_Y and UTS values that were 2.2- and 2.6-fold those of controls, respectively. In terms of the native-to-native assemblies, histological evaluation showed little to no integration in either control or LOX-treated groups, which was further confirmed biomechanically (Fig. 4D–F). Interestingly, results further revealed the integration interface in LOX-treated engineered-to-native assembles to have ~7.5-fold greater tensile stiffness and strength compared to those of LOX-treated native-to-native assemblies.

3.3. Phase 3: *In vivo* integration of native and engineered fibrocartilage

At 6 wk post-surgery, the mice were humanely sacrificed, and the tissue assemblies were harvested and analyzed histologically and biomechanically. Histological evaluation of the engineered-to-native assemblies post-sacrifice revealed untreated assemblies to be insufficiently integrated; both the single and double LOX treatments, however, were found to promote more complete fusion of the integration interface. Further, the neofibrocartilage in the double LOX-treated assemblies presented with denser collagen staining compared to the engineered tissue in single LOX-treated assemblies (Fig. 5A). Biomechanical testing found both LOX treatments to significantly increase the tensile stiffness and strength of the integration interface compared to untreated assemblies (Fig. 5B–C). Specifically, the E_Y and UTS of the integration interface in single LOX-treated assemblies were 3.3- and 3.2-fold, respectively, those of controls. The double LOX treatment, on the other hand, increased the E_Y and UTS of the integration interface 4.3- and 4.7-fold control values, respectively. Analysis was also conducted to compare the *in vitro* integration results of Phase 2 with the *in vivo* results of Phase 3 (Fig. 5D–E). A two-tailed, paired Student's *t*-test revealed the *in vivo* double LOX treatment to promote significantly enhanced E_Y and UTS values that were 304% and 230% greater, respectively, than those achieved in combination-treated constructs *in vitro.* In comparing the E_Y and UTS of the integration interface of *in vivo* double LOX-treated assemblies to *in vitro* control assemblies revealed 730% and 745% significant increases, respectively, in the combination-treated *in vivo* assemblies over *in vitro* controls. No significant differences, however, were observed between *in vitro* and *in vivo* controls. Further, two-way ANOVA analysis found both the LOX+C-ABC+TGF-β1 pre-treatment as well as the *in vivo* subcutaneous environment to be significant factors toward enhancing the integration interface stiffness and strength in fibrocartilaginous engineered-to-native assemblies.

4. Discussion

In light of the current insufficiencies of fibrocartilage implants, this study sought to enhance the biomechanical integrity of neofibrocartilage as well as to facilitate and stabilize their

integration with native tissue via a combination of stimuli: LOX, C-ABC, and TGF-β1. Innovative aspects of this study include finding that the LOX+C-ABC+TGF-β1 treatment 1) enhances the tensile properties of self-assembled fibrocartilage via time-dependent maturation of the neotissue's ECM, and 2) promotes integration between engineered and host tissues in an animal model. This study also demonstrates that LOX is a potent agent for enhancing integration between native-to-implant surfaces, confirming the pivotal role of PYR crosslinks at the integration interface. Furthermore, this work shows, for the first time, that a pre-treatment carries over an effect into an *in vivo* model achieving functional integration. Methods used in this study were able to address the two most cumbersome factors that currently hinder integration, including cell death at the wound edge and the lack of collagen crosslinks at the integration interface. Thus, using self-assembled neofibrocartilage implants allows for implantation of highly cellular, metabolically active implants that, when treated with LOX+C-ABC+TGF-β1, are primed for enhanced integration potential following implantation toward achieving values on par with intact native fibrocartilage.

Phase 1 of this study established that longer culture duration post-LOX application promotes a more biomechanically robust matrix. While the 12 wk time point was found to be a significant factor toward enhancing neotissue tensile properties, it was not a significant factor toward enhancing collagen content. Previous work has shown that as highly collagenous native tissues develop and mature, the density and diameters of their collagen fibrils increase, along with increased fibrillar bundling and matrix compaction; together, these structural modifications translate to a matrix capable of withstanding greater tensile loading [28–30]. Similarly, the present study found the 12 wk time point to be a significant factor toward increasing the collagen fibril diameter and density in LOX+C-ABC+TGF-β1-treated constructs, as well as to promote distinct collagen bundling. Thus, results indicate that, over time, the LOX+C-ABC+TGF-β1 treatment promotes *in vitro* neofibrocartilage maturation similar to the maturation observed during native tissue morphogenesis, resulting in neofibrocartilage with greater tensile properties.

Concurrent with the observed matrix modifications, neofibrocartilage treated with LOX+C-ABC+TGF-β1 also experienced increased intramolecular collagen crosslink content. While no significant difference in crosslink content was observed between LOX- and LOX+C-ABC+TGF-β1-treated constructs at t = 6 wk, by t = 12 wk, the crosslink content in combination-treated constructs was significantly increased over all other groups. It has been shown that LOX-mediated PYR collagen crosslinks take ~7 – 30 d to fully mature [23]. While no significant differences were observed in PYR content in 6 wk vs. 12 wk time points, it is, therefore, likely that the longer culture duration allowed for the development of more mature PYR crosslinks to form. Previous work has indicated that it is specifically the mature crosslinks that are correlated with the tensile robustness of native musculoskeletal tissues [31, 32]. With more time for the crosslinks to mature *in vitro*, constructs receiving LOX and grown to 12 wk were better suited to withstand tensile loads. Combining LOX with C-ABC+TGF-β1, therefore, neofibrocartilage grown to 12 wk had the benefits of all three agents, including 1) increased collagen content as an anabolic result of TGF-β1, 2) a compacted collagen matrix having greater fibril diameters as a result of GAG depletion by

C-ABC, and 3) more mature PYR crosslinks, mediated by LOX, that aided in the bundling of fibrils into more mechanically robust fibers. Thus, results indicate that the increased tensile properties are directly related to matrix maturation, organization, and crosslinking, showing combined use of these three agents to be a potent regimen to promote matrix maturation and enhanced neotissue biomechanical integrity over time (Fig. 6).

LOX was found to promote integration between neofibrocartilage and native tissue in Phase 2's *in vitro* model, using the treatment regimen established in Phase 1. Specifically, the integration interface stiffness and strength were significantly increased an average of 114% and 148%, respectively, in engineered-to-native assemblies treated with either LOX alone or with LOX+C-ABC+TGF-β1. The finding that the LOX+C-ABC+TGF-β1 treatment regimen did not promote integration significantly more than LOX alone suggests that LOX is the crucial factor contributing to the enhanced integration potential of neofibrocartilage. This indicates that increased PYR collagen crosslinks are critical to the formation of a more robust integration interface. Previous work has found β-aminopropionitrile, an agent that irreversibly inhibits LOX activity, thus blocking collagen crosslink formation, to inhibit integration between hyaline cartilage explants [33], further showing the importance of crosslinks at the integration interface. Thus, results of the present study show that using exogenous LOX to upregulate PYR crosslink formation not only aids in promoting maturation of the neotissue along with C-ABC and TGF-β1, but is also integral toward facilitating and stabilizing the integration interface between engineered implants and native tissue (Fig. 6).

The engineered-to-native assemblies produced a significantly stronger integration interface than the native-to-native assemblies, as seen in Phase 2. While LOX treatment doubled the tensile stiffness of the interface of native-to-native assemblies compared to untreated native-to-native controls, the effect of LOX was 7.5-fold larger toward enhancing the tensile properties of engineered-to-native assemblies. Natively, collagen crosslinks in fibrocartilaginous tissues remain in an unstable, immature, reducible form during early development; however, as the tissue matures, these reducible crosslinks are converted into more stable, mature, non-reducible PYR crosslinks [34]. Thus, the low cellularity and highly dense, mature crosslink-stabilized matrix likely inhibited exogenous LOX from having much effect at promoting integration in native-to-native assemblies [7, 10]. This suggests that the high cellularity, immature collagen matrix, and high collagen crosslinking potential of the self-assembled constructs enabled the neofibrocartilage to better respond to LOX, resulting in the formation of PYR crosslinks at the integration interface. Over time in culture, therefore, the metabolically active integration interface in engineered-to-native assemblies matured to produce significantly stronger bonding than in the metabolically inactive native-to-native assemblies.

In vivo implantation of the native-to-engineered tissue carried over and significantly enhanced the LOX-mediated integration effects. This was identified in the final phase in which fibrocartilage, pre-treated with a double LOX application in addition to C-ABC +TGF-β1, promoted greater integration between native and engineered fibrocartilage. Specifically, this treatment increased the integration interface E_Y and UTS by 4.3- and 4.7-fold, respectively, than values achieved in untreated implant assemblies. Further, when

compared to integration values achieved using the same treatment *in vitro*, the *in vivo* environment was found to improve the integration interface tensile stiffness and strength by 304% and 230%, respectively. These significant enhancements are likely attributable to the nutrient rich environment and mechanical stresses placed on the engineered-to-native assemblies in the subcutaneous environment [27, 35, 36]. However, because no significant differences were found between the integration properties of *in vitro* and *in vivo* control assemblies, the 4.1-fold significant enhancement in the integration properties of LOX+C-ABC+TGF-β1-treated *in vivo* compared to *in vitro* engineered-to-native assemblies indicates the subcutaneous environment had a more potent effect in the pre-treated neofibrocartilage. Thus, the pre-treatment likely primed the implant to better respond to the *in vivo* environment, further accelerating its maturation and, hence, interfacial integration with native tissue (Fig. 6). This speaks to the potential for LOX+C-ABC+TGF-β1-treated neofibrocartilage implants to further mature and form even more stable integration interfaces given longer *in vivo* culture time. Future work must therefore investigate the effects of this treatment toward promoting long-term integration in functional defect sites *in vivo*.

Of the few studies that have mechanically characterized the integration interface in fibrocartilaginous repair models [37, 38], only one study has utilized a pull-to-failure test similar to the test used in the present study. This study generated electrospun nanofibrous scaffolds containing entrapped collagenase, with the goal of locally controlling matrix degradation at the meniscus wound interface to enhance native-to-native tissue repair. Results found the integration interface tensile strength to trend higher in defects containing the collagenase-releasing scaffold compared to empty defects or those containing non-collagenase-releasing scaffolds following 50 d of *in vitro* culture, with the integration interface tensile strength of the best group averaging at 13.5 kPa [39]. The present study similarly found the integration interface tensile strength to trend higher in LOX-treated native-to-native assemblies, with a value of 25.9 kPa. Use of the LOX+C-ABC+TGF-β1 and the highly cellular neotissue in engineered-to-native assemblies, however, resulted in integration E_Y values of 240 kPa following *in vitro* culture, which were further promoted following *in vivo* culture to 890 kPa. In comparing the achieved integration interface tensile modulus to those of intact fibrocartilaginous tissues, results of the *in vivo* portion of this study indicate that the integration interface in assemblies containing LOX+C-ABC+TGF-β1-treated neofibrocartilage was ~100% of the tensile modulus of intact intervertebral disc anulus fibrosus tissue in the axial direction [40], ~28% of intact native TMJ disc middle zone tissue in the mediolateral direction [41], and ~18% of intact native meniscal tissue in the radial direction [42]. Thus, results indicate this combination treatment significantly improves the integration robustness of engineered fibrocartilage implants to values on par with those of intact native tissue.

5. Conclusions

In summary, this study addresses the current insufficiencies of fibrocartilage implants, namely their subpar biomechanical integrity and, more importantly, their inability to integrate with native tissue upon implantation. Specifically, this study shows that a LOX+C-ABC+TGF-β1 pre-treatment regimen synergistically enhances the biomechanical functionality and primes the integration of highly cellularized, metabolically active, self-

assembled neofibrocartilage. By addressing two of the most difficult factors that currently inhibit integration, the tensile properties of the integration interface achieved *in vivo* were on par with values of intact native fibrocartilage. Methods developed in this study are translatable toward addressing defects in a wide variety of fibrocartilaginous tissues. Future work will be focused on adapting these methods toward further promoting the functional properties and integration potential of neofibrocartilage in site-specific, large animal fibrocartilage defect models.

Acknowledgments

The authors would like to acknowledge funding support from NIH 5-T32-GM008799, R01 AR053286, and R01 DE019666.

References

1. Kawamura S, Lotito K, Rodeo SA. Biomechanics and healing response of the meniscus. Oper Tech Sports Med. 2003; 11:68–76.
2. Gebremariam L, Koes BW, Peul WC, Huisstede BM. Evaluation of treatment effectiveness for the herniated cervical disc: a systematic review. Spine. 2012; 37:E109–E118. [PubMed: 21587105]
3. Hunziker EB. Biologic repair of articular cartilage. Defect models in experimental animals and matrix requirements. Clin Orthop Relat Res. 1999:S135–S146. [PubMed: 10546642]
4. Khan IM, Gilbert SJ, Singhrao SK, Duance VC, Archer CW. Cartilage integration: evaluation of the reasons for failure of integration during cartilage repair. A review. Eur Cell Mater. 2008; 16:26–39. [PubMed: 18770504]
5. Huey DJ, Hu JC, Athanasiou KA. Unlike bone, cartilage regeneration remains elusive. Science. 2012; 338:917–921. [PubMed: 23161992]
6. Benjamin M, Ralphs JR. Biology of fibrocartilage cells. Int Rev Cytol. 2004; 233:1–45. [PubMed: 15037361]
7. Hunziker EB, Quinn TM. Surgical removal of articular cartilage leads to loss of chondrocytes from cartilage bordering the wound edge. J Bone Joint Surg Am. 2003; 85-A(Suppl 2):85–92. [PubMed: 12721349]
8. Ionescu LC, Lee GC, Garcia GH, Zachry TL, Shah RP, Sennett BJ, et al. Maturation state-dependent alterations in meniscus integration: implications for scaffold design and tissue engineering. Tissue Eng Part A. 2011; 17:193–204. [PubMed: 20712419]
9. Woo SL, Vogrin TM, Abramowitch SD. Healing and repair of ligament injuries in the knee. J Am Acad Orthop Surg. 2000; 8:364–372. [PubMed: 11104400]
10. Bos PK, DeGroot J, Budde M, Verhaar JA, van Osch GJ. Specific enzymatic treatment of bovine and human articular cartilage: implications for integrative cartilage repair. Arthritis Rheum. 2002; 46:976–985. [PubMed: 11953975]
11. Jurgensen K, Aeschlimann D, Cavin V, Genge M, Hunziker EB. A new biological glue for cartilage-cartilage interfaces: tissue transglutaminase. J Bone Joint Surg Am. 1997; 79:185–193. [PubMed: 9052538]
12. Scotti C, Pozzi A, Mangiavini L, Vitari F, Boschetti F, Domeneghini C, et al. Healing of meniscal tissue by cellular fibrin glue: an in vivo study. Knee Surg Sports Traumatol Arthrosc. 2009; 17:645–651. [PubMed: 19296087]
13. Hunziker EB, Kapfinger E. Removal of proteoglycans from the surface of defects in articular cartilage transiently enhances coverage by repair cells. J Bone Joint Surg Br. 1998; 80:144–150. [PubMed: 9460972]
14. Takegami K, An HS, Kumano F, Chiba K, Thonar EJ, Singh K, et al. Osteogenic protein-1 is most effective in stimulating nucleus pulposus and annulus fibrosus cells to repair their matrix after chondroitinase ABC-induced in vitro chemonucleolysis. Spine J. 2005; 5:231–238. [PubMed: 15863076]

15. Hu JC, Athanasiou KA. A self-assembling process in articular cartilage tissue engineering. Tissue Eng. 2006; 12:969–979. [PubMed: 16674308]
16. Hoben GM, Hu JC, James RA, Athanasiou KA. Self-assembly of fibrochondrocytes and chondrocytes for tissue engineering of the knee meniscus. Tissue Eng. 2007; 13:939–946. [PubMed: 17484700]
17. Ofek G, Revell CM, Hu JC, Allison DD, Grande-Allen KJ, Athanasiou KA. Matrix development in self-assembly of articular cartilage. PLoS One. 2008; 3:e2795. [PubMed: 18665220]
18. Kalpakci KN, Kim EJ, Athanasiou KA. Assessment of growth factor treatment on fibrochondrocyte and chondrocyte co-cultures for TMJ fibrocartilage engineering. Acta Biomater. 2011; 7:1710–1718. [PubMed: 21185408]
19. Huey DJ, Athanasiou KA. Maturational growth of self-assembled, functional menisci as a result of TGF-beta1 and enzymatic chondroitinase-ABC stimulation. Biomaterials. 2011; 32:2052–2058. [PubMed: 21145584]
20. MacBarb RF, Makris EA, Hu JC, Athanasiou KA. A chondroitinase-ABC and TGF-beta1 treatment regimen for enhancing the mechanical properties of tissue-engineered fibrocartilage. Acta Biomater. 2013; 9:4626–4634. [PubMed: 23041782]
21. Macbarb RF, Chen AL, Hu JC, Athanasiou KA. Engineering functional anisotropy in fibrocartilage neotissues. Biomaterials. 2013; 34:9980–9989. [PubMed: 24075479]
22. Makris EA, Hu JC, Athanasiou KA. Hypoxia-induced collagen crosslinking as a mechanism for enhancing mechanical properties of engineered articular cartilage. Osteoarthritis Cartilage. 2013; 21:634–641. [PubMed: 23353112]
23. Ahsan T, Harwood F, McGowan KB, Amiel D, Sah RL. Kinetics of collagen crosslinking in adult bovine articular cartilage. Osteoarthritis Cartilage. 2005; 13:709–715. [PubMed: 16043034]
24. Wang SX, Mure M, Medzihradszky KF, Burlingame AL, Brown DE, Dooley DM, et al. A crosslinked cofactor in lysyl oxidase: redox function for amino acid side chains. Science. 1996; 273:1078–1084. [PubMed: 8688089]
25. Athens AA, Makris EA, Hu JC. Induced collagen cross-links enhance cartilage integration. PLoS One. 2013; 8:e60719. [PubMed: 23593295]
26. Makris EA, MacBarb RF, Responte DJ, Hu JC, Athanasiou KA. A copper sulfate and hydroxylysine treatment regimen for enhancing collagen cross-linking and biomechanical properties in engineered neocartilage. FASEB J. 2013; 27:2421–2430. [PubMed: 23457219]
27. Responte DJ, Arzi B, Natoli RM, Hu JC, Athanasiou KA. Mechanisms underlying the synergistic enhancement of self-assembled neocartilage treated with chondroitinase-ABC and TGF-beta1. Biomaterials. 2012; 33:3187–3194. [PubMed: 22284584]
28. Ahn HJ, Paik SK, Choi JK, Kim HJ, Ahn DK, Cho YS, et al. Age-related changes in the microarchitecture of collagen fibrils in the articular disc of the rat temporomandibular joint. Arch Histol Cytol. 2007; 70:175–181. [PubMed: 18079586]
29. Diamant J, Keller A, Baer E, Litt M, Arridge RG. Collagen; ultrastructure and its relation to mechanical properties as a function of ageing. Proc R Soc Lond B Biol Sci. 1972; 180:293–315. [PubMed: 4402469]
30. Parry DA. The molecular and fibrillar structure of collagen and its relationship to the mechanical properties of connective tissue. Biophys Chem. 1988; 29:195–209. [PubMed: 3282560]
31. Eleswarapu SV, Responte DJ, Athanasiou KA. Tensile properties, collagen content, and crosslinks in connective tissues of the immature knee joint. PLoS One. 2011; 6:e26178. [PubMed: 22022553]
32. Frank C, McDonald D, Wilson J, Eyre D, Shrive N. Rabbit medial collateral ligament scar weakness is associated with decreased collagen pyridinoline crosslink density. J Orthop Res. 1995; 13:157–165. [PubMed: 7722752]
33. Ahsan T, Lottman LM, Harwood F, Amiel D, Sah RL. Integrative cartilage repair: inhibition by beta-aminopropionitrile. J Orthop Res. 1999; 17:850–857. [PubMed: 10632452]
34. Fujimoto D, Moriguchi T. Pyridinoline, a non-reducible crosslink of collagen. Quantitative determination, distribution, and isolation of a crosslinked peptide. J Biochem. 1978; 83:863–867. [PubMed: 641035]

35. Calve S, Lytle IF, Grosh K, Brown DL, Arruda EM. Implantation increases tensile strength and collagen content of self-assembled tendon constructs. J Appl Physiol. 2010; 108:875–881. (1985). [PubMed: 20110546]

36. Wang B, Liu W, Zhang Y, Jiang Y, Zhang WJ, Zhou G, et al. Engineering of extensor tendon complex by an ex vivo approach. Biomaterials. 2008; 29:2954–2961. [PubMed: 18423583]

37. Ionescu LC, Mauck RL. Porosity and cell preseeding influence electrospun scaffold maturation and meniscus integration in vitro. Tissue Eng Part A. 2013; 19:538–547. [PubMed: 22994398]

38. Ionescu LC, Lee GC, Huang KL, Mauck RL. Growth factor supplementation improves native and engineered meniscus repair in vitro. Acta Biomater. 2012; 8:3687–3694. [PubMed: 22698946]

39. Qu F, Lin JM, Esterhai JL, Fisher MB, Mauck RL. Biomaterial-mediated delivery of degradative enzymes to improve meniscus integration and repair. Acta Biomater. 2013; 9:6393–6402. [PubMed: 23376132]

40. Elliott DM, Setton LA. Anisotropic and inhomogeneous tensile behavior of the human anulus fibrosus: experimental measurement and material model predictions. J Biomech Eng. 2001; 123:256–263. [PubMed: 11476369]

41. Beatty MW, Bruno MJ, Iwasaki LR, Nickel JC. Strain rate dependent orthotropic properties of pristine and impulsively loaded porcine temporomandibular joint disk. J Biomed Mater Res. 2001; 57:25–34. [PubMed: 11416845]

42. Tissakht M, Ahmed AM. Tensile stress-strain characteristics of the human meniscal material. J Biomech. 1995; 28:411–422. [PubMed: 7738050]

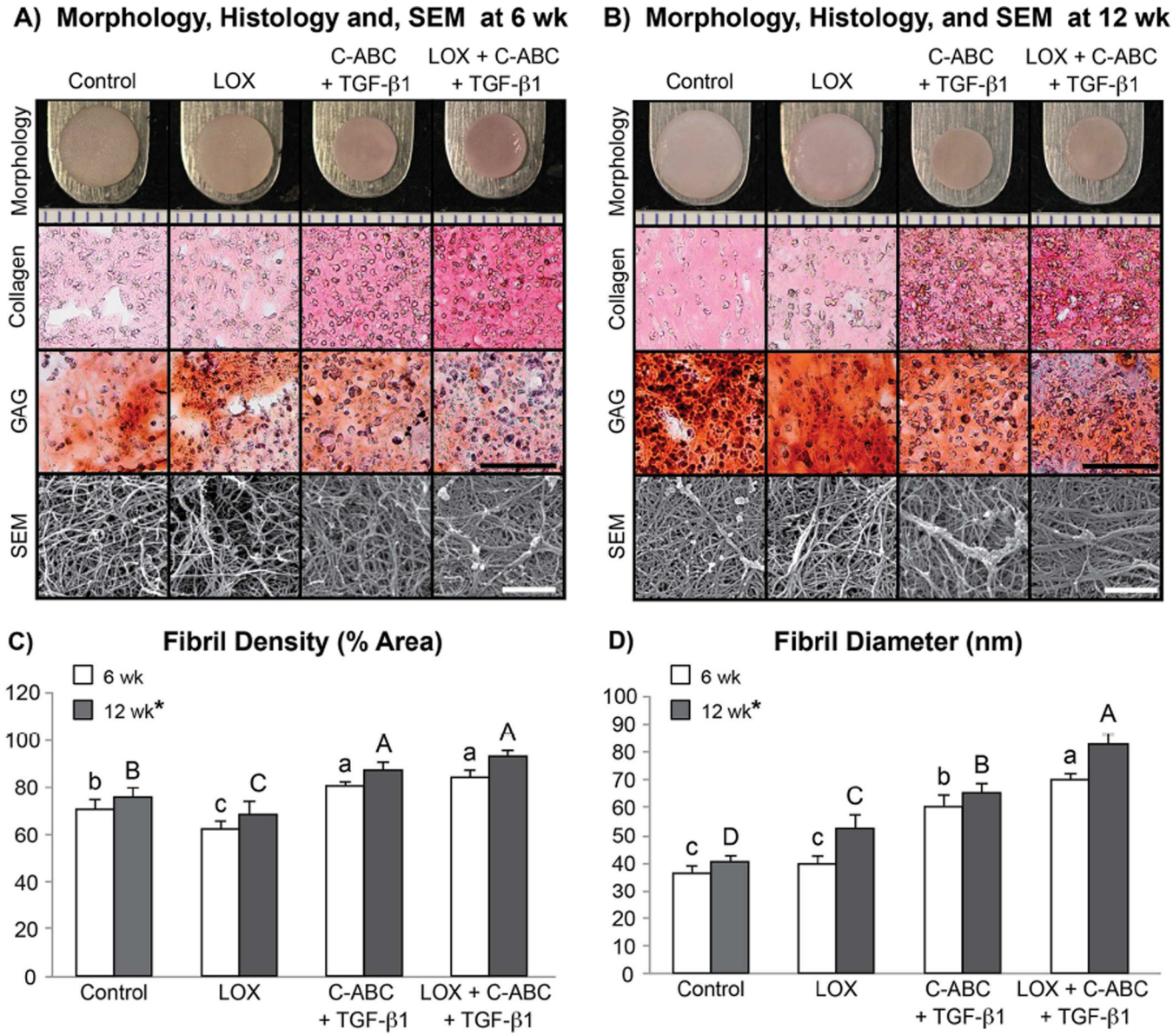

Fig. 1.

Phase 1 gross morphology (markings on ruler = 1 mm), Picrosirius Red for collagen and Safranin O/Fast Green for sulfated glycosaminoglycans (GAG) stained sections (scale bar = 100 μm), and representative scanning electron microscopy (SEM) images (scale bar = 1 μm) of untreated, LOX, C-ABC+TGF-β1, and LOX+C-ABC+TGF-β1 neofibrocartilage at t = 6 wk (*A*) and t = 12 wk (*B*). Collagen fibril density (*C*) and diameter (*D*) quantified from SEM images, bars not connected by the same letter are significantly different ($p < 0.05$), lower case letters denote significant differences for 6 wk constructs, upper case letters denote significant differences for 12 wk constructs, $n = 6$ per group, mean ± SD.

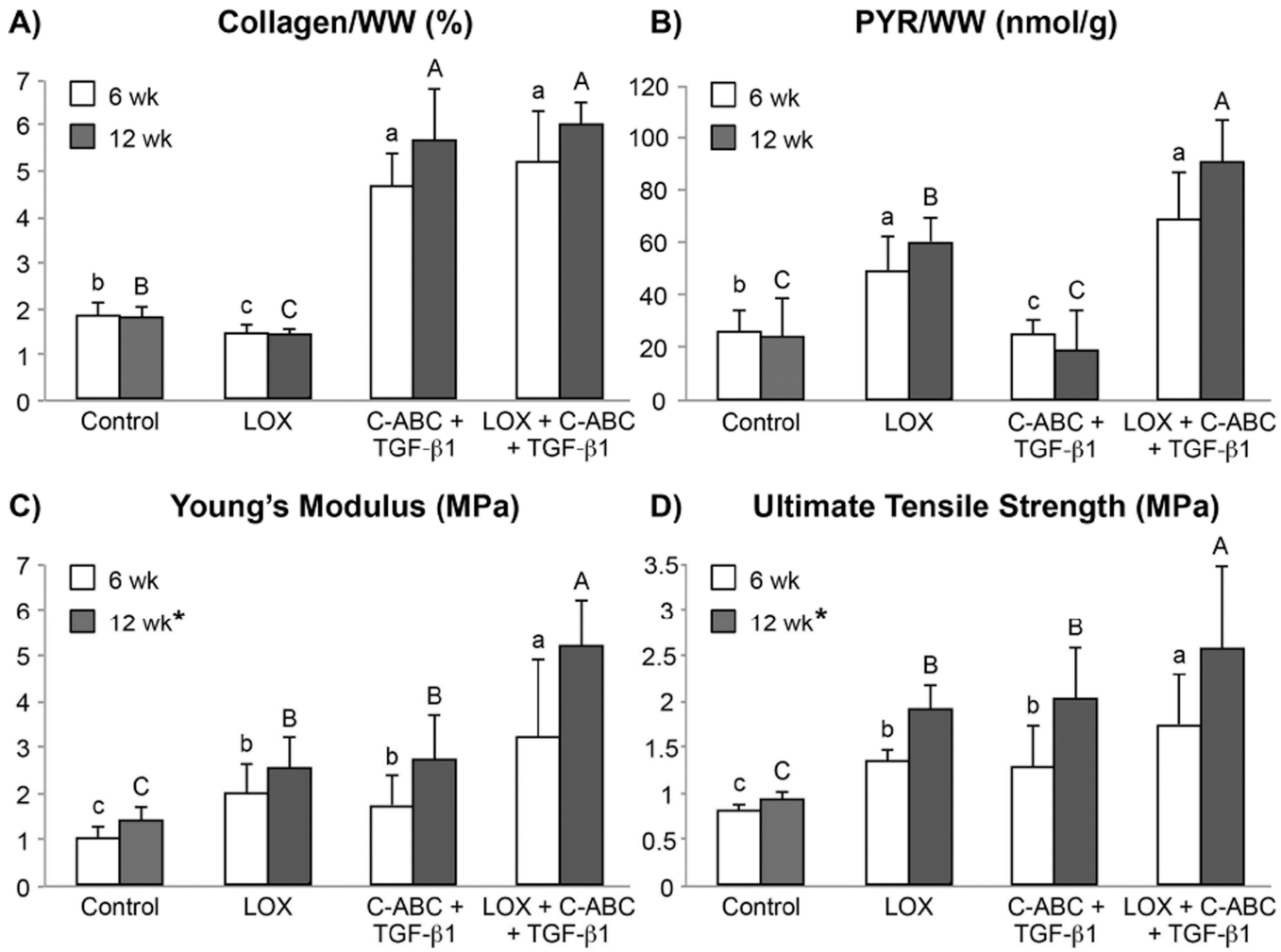

Fig. 2. Phase 1 Neotissue Functional Properties at t = 6 and 12 wk

Collagen content per construct wet weight (*A*), pyridinoline content per construct wet weight (*B*), Young's modulus (*C*), and ultimate tensile strength (*D*) of untreated, LOX, C-ABC +TGF-β1, and LOX+C-ABC+TGF-β1 neofibrocartilage at t = 6 and 12 wk. Bars not connected by the same letter are significantly different ($p < 0.05$), lower case letters denote significant differences for 6 wk constructs, upper case letters denote significant differences for 12 wk constructs, $n = 6$ per group, mean ± SD.

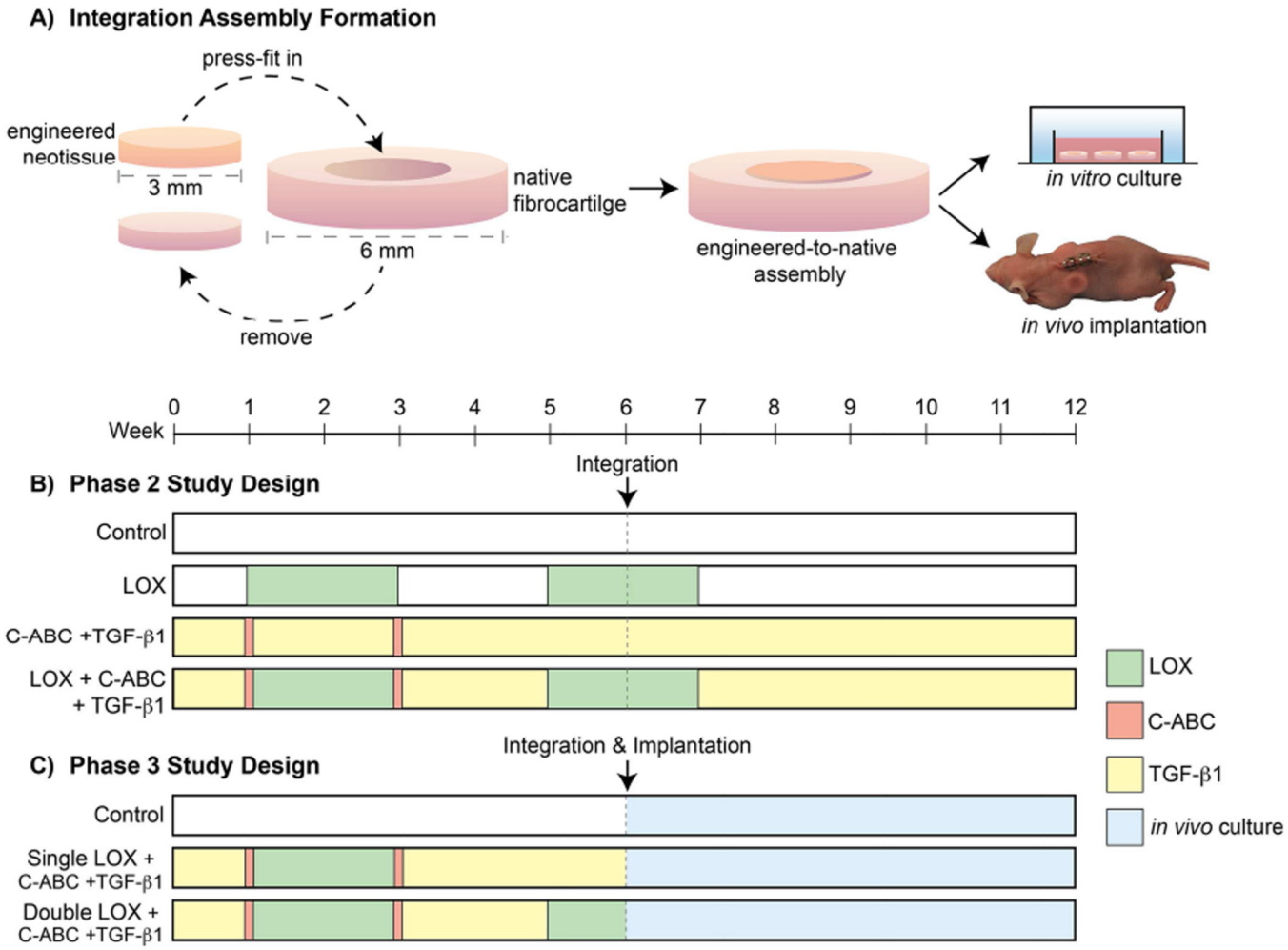

Fig. 3. Phase 2 and 3 Experimental Designs

A fibrocartilage defect model was formed by press fitting 3 mm punches of 6-wk-old neofibrocartilage into same-size native fibrocartilage defects and grown either *in vitro* or *in vivo* for an additional 6 wk (*A*). Control (none), LOX, C-ABC+TGF-β1, or LOX+C-ABC +TGF-β1 pre-treatments were applied to neofibrocartilage prior to integration assembly formation and *in vitro* culture in Phase 2 (*B*). Control (none), single LOX+C-ABC+TGF-β1, or double LOX+C-ABC+ TGF-β1 pre-treatments were applied to neofibrocartilage prior to integration assembly formation and *in vivo* culture in the backs of athymic mice in Phase 3 (*C*).

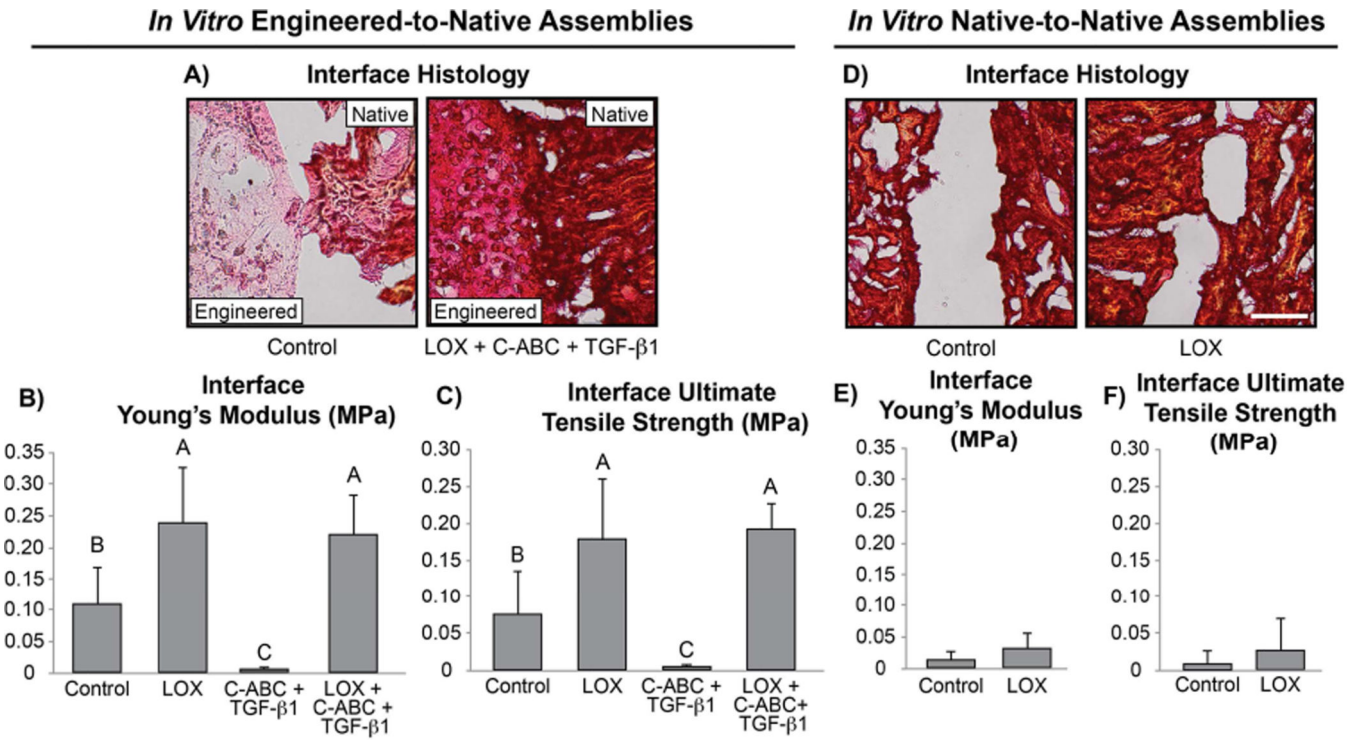

Fig. 4. Phase 2 *In Vitro* Integration Interface Histology and Tensile Properties

Picrosirius Red (for collagen) stained integration interface sections for control and LOX+C-ABC+TGF-β1 pre-treated engineered-to-native assemblies (*A*) (scale bar = 100 μm). Interface Young's modulus (*B*) and ultimate tensile strength (*C*) of control, LOX, C-ABC +TGF-β1, and LOX+C-ABC+TGF-β1 pre-treated engineered-to-native assemblies. Picrosirius Red (for collagen) stained integration interface sections for control and LOX-treated native-to-native assemblies (*D*) (scale bar = 100 μm). Interface Young's modulus (*E*) and ultimate tensile strength (*F*) of control and LOX treated native-to-native assemblies. Bars not connected by the same letter are significantly different ($p < 0.05$), $n = 6$ per group, mean ± SD.

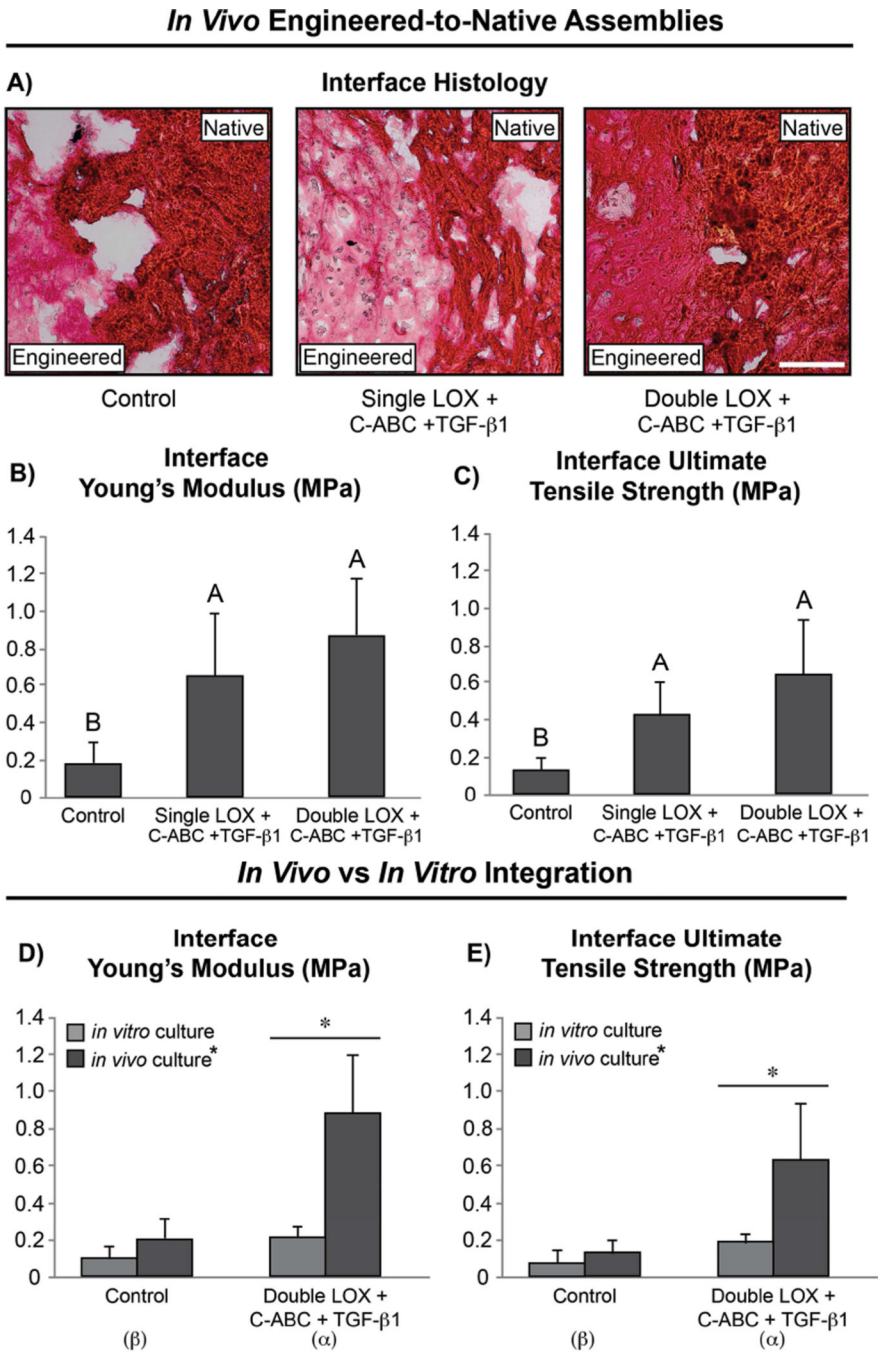

Fig. 5. Phase 3 *In Vivo* Integration Interface Histology and Tensile Properties; Comparison with Phase 2 *In Vitro* Results

Picrosirius Red (for collagen) stained integration interface sections (*A*) (scale bar = 100 μm), interface Young's modulus (*B*), and ultimate tensile strength (*C*) of control, single LOX+C-ABC+TGF-β1, and double LOX+C-ABC+TGF-β1 pre-treated engineered-to-native assemblies. Bars not connected by the same letter are significantly different ($p < 0.05$), $n = 6$ per group, mean ± SD. Comparison between Phase 2 (*in* vitro) and Phase 3 (*in vivo*) results for interface Young's modulus (*D*) and ultimate tensile strength (*E*). Asterix represents

significance between *in vitro* and *in vivo* results, and Greek letters represent significance between control and LOX+C-ABC+TGF-β1 treatment following 2-way ANOVA analysis, $n = 6$ per group, mean ± SD.

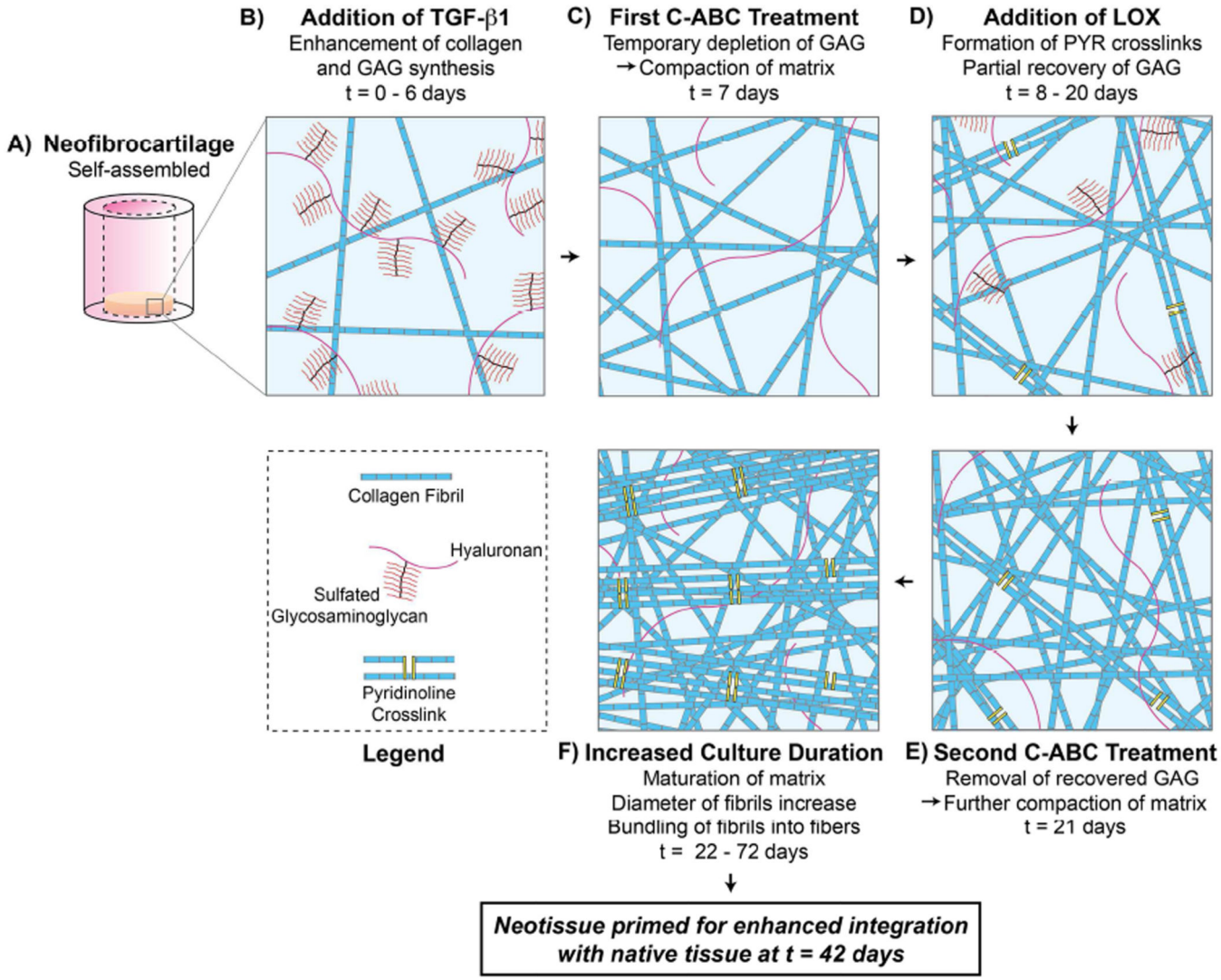

Fig. 6. Neofibrocartilage Matrix Maturation, Organization, and Crosslinking following LOX+C-ABC+TGF-β1 Pre-treatment

Following self-assembly of neofibrocartilage (*A*), neotissue is grown in the presence of TGF-β1 starting at t = 0 days (*B*), promoting matrix synthesis. The first C-ABC treatment at t = 7 days (*C*) temporarily depletes glycosaminoglycan (GAG) content and compacts the matrix. LOX is added from t = 8 to 20 days (*D*), resulting in pyridinoline (PYR) crosslink formation, while GAG partially recovers. The second C-ABC treatment at t = 21 days (*E*) removes any recovered GAG, furthering compacting the matrix. Increased *in vitro* culture duration of the neotissue to t = 72 days results in matrix maturation and bundling of fibrils into fibers (*F*). Together, these treatments, in addition to a second LOX treatment (Phases 2 and 3), prime the neofibrocartilage matrix for enhanced integration potential with native tissue by t = 42 days.

Table 1

Phase 1 Neotissue Gross Morphological and Compressive Properties at t = 6 and 12 wk

Values are provided for t = 6 wk (top) and t = 12 wk (bottom). Values marked with different letters within each category are significantly different ($p < 0.05$), $n = 6$ per group, with A > B > C.

6 wk constructs	Wet weight (mg)	Hydration (%)	Diameter (mm)	Thickness (mm)	GAG/WW (%)	E_r (kPa)	E_i (kPa)
Control	13.54 ± 0.39^{A}	87.48 ± 1.32^{A}	5.49 ± 0.04^{A}	0.61 ± 0.06^{A}	5.97 ± 0.41^{A}	42.59 ± 2.49^{B}	228.66 ± 59.92^{B}
LOX	12.75 ± 0.36^{A}	86.18 ± 1.25^{A}	5.53 ± 0.10^{A}	0.48 ± 0.07^{B}	6.89 ± 0.81^{A}	75.74 ± 47.98^{A}	652.17 ± 218.19^{A}
C-ABC + TGF-β1	6.75 ± 0.17^{B}	81.95 ± 2.75^{B}	4.55 ± 0.07^{B}	0.42 ± 0.05^{C}	2.94 ± 0.42^{B}	14.18 ± 2.90^{C}	240.67 ± 67.42^{B}
LOX + C-ABC + TGF-β1	6.51 ± 0.23^{B}	80.45 ± 3.88^{B}	4.55 ± 0.03^{B}	0.42 ± 0.03^{C}	1.83 ± 0.48^{C}	14.26 ± 5.11^{C}	230.01 ± 87.84^{B}
12 wk constructs	**Wet weight (mg)**	**Hydration (%)**	**Diameter (mm)**	**Thickness (mm)**	**GAG/WW (%)**	**E_r (kPa)**	**E_i (kPa)**
Control	22.76 ± 1.99^{A}	84.19 ± 1.54^{A}	6.22 ± 0.09^{A}	0.70 ± 0.14^{B}	11.00 ± 1.28^{A}	220.24 ± 51.01^{A}	$443.62 \pm 231.04A^{B}$
LOX	21.08 ± 1.24^{A}	83.29 ± 2.20^{A}	5.89 ± 0.08^{A}	0.74 ± 0.03^{A}	10.30 ± 1.08^{A}	268.21 ± 117.19^{A}	823.72 ± 178.73^{A}
C-ABC + TGF-β1	7.68 ± 1.73^{B}	81.73 ± 1.06^{B}	4.51 ± 0.14^{B}	0.49 ± 0.05^{C}	2.59 ± 1.21^{B}	19.92 ± 9.54^{B}	277.66 ± 115.61^{B}
LOX + C-ABC + TGF-β1	6.32 ± 0.15^{B}	80.16 ± 0.70^{B}	4.58 ± 0.01^{B}	0.48 ± 0.03^{C}	0.65 ± 0.56^{C}	7.23 ± 8.88^{B}	120.77 ± 38.51^{C}